JOURNAL OF SCIENCE
SAKARYA UNIVERSITY

Sakarya University Journal of Science

ISSN 1301-4048 | e-ISSN 2147-835X | Period Bimonthly | Founded: 1997 | Publisher Sakarya University | http://www.saujs.sakarya.edu.tr/

Title: Comparative Study about Differently Structured Transitional Metal Molybdates as Negative Electrodes for LIBs

Authors: Billur Deniz Karahan
Recieved: 2019-07-29 16:24:14

Accepted: 2019-10-10 13:54:16

Article Type: Research Article
Volume: 24
Issue: 1
Month: February
Year: 2020
Pages: 67-77

How to cite
Billur Deniz Karahan; (2020), Comparative Study about Differently Structured Transitional Metal Molybdates as Negative Electrodes for LIBs . Sakarya University Journal of Science, 24(1), 67-77, DOI: 10.16984/saufenbilder.598141
Access link
http://www.saujs.sakarya.edu.tr/tr/issue/49430//598141

Sakarya University Journal of Science 24(1), 67-77, 2020

Comparative Study about Differently Structured Transitional Metal Molybdates as Negative Electrodes for LIBs

Billur Deniz Karahan[1]

Abstract

The nanostructured materials represent the center of fundamental advances to design new era electrodes for high energy density batteries. Especially, one-dimensional nanomaterials are recognized as a solution due to their large surface area, short diffusion distance and high volume accommodation ability. In this sense, first in literature a comparative study has been done to examine the electrochemical performances of differently fabricated transition metal oxide molybdate powders: lithium storage capabilities of nickel-cobalt-molybdate composite is compared to that of the cobalt oxide decorated nickel molybdate powders. To measure the effect of cobalt atom, bare nickel molybdate powders have been also fabricated and tested. The lithiation mechanism of these electrodes are discussed based on the cyclic voltammetry curvatures. SEI layer formation on the electrodes and the electrode/electrolyte stability upon cycling are analyzed following the electrochemical impedance spectroscopy test results (after 1st, 2nd and 4th cycles). The results reveal that the addition of cobalt changes the powder morphology and improves the electrochemical performance of the electrode. Among three samples, the cobalt oxide decorated nickel molybdate performs higher retention and rate performance since the top layer promotes more stable electrode/electrolyte interface providing a capacity of 290 mAh/g after 100 cycles. The rate performance of the sample is also found promising, the electrode delivers 200 mAh/g even under a current load of 400mA/g.

Keywords: Metal molybdates, lithium ion batteries, hydrothermal method, anode

1. INTRODUCTION

Recently, as LIBs become the most preferred technology for the world of portable electronic devices, designing new electrodes with higher energy and power densities attract attention. In this concept, transitional metal oxides (TMOs) become the subject of extensive researches because of their high theoretical capacities. Among them, transitional metal molybdates stand out due to molybdenum's various oxidation states (from 4+ to 6+), its natural abundance, high electrochemical activity and ability to deliver high capacities at potentials lower than 2V [1,2]. Herein, the stable crystal structure of molybdates, their redox behaviors and remarkable physical/chemical properties highlight their possible uses in energy-storage field applications.

[1] Istanbul Medipol University, Istanbul, Turkey ORCID: 0000-0002-7839-2222 – bdkarahan@medipol.edu.tr

Literature review demonstrates that molybdenum oxides electrodes are not commercialized because of the kinetic problems caused by their inadequate intrinsic conductivies, slow solid state Li diffusion and destructive volume changes that happen upon cycling. Plus, in most cases these electrodes fail in early cycles due to irreversible phase transformations occurred upon cycling. Then in 2004, Leyzerovich et al [3] have proposed the use of mixed-molybdenum oxides as electrodes in LIBs. They have claimed that the combination of two metals in oxide matrix creates a new material, different than the binary oxides. In this sense, $NiMoO_4$ has been investigated due to its electrical conductivity (10^{-6} S cm^{-1}) which is higher than that of the bare NiO [4]. Although, its rate capability is still considered to be very low to be used as electrode material in practical applications the cycle life is noted to be improved in reference to the pure molybdate oxide electrodes. Alternatively, $CoMoO_4$ has been studied as electrode material because of its excellent rate capability as Mo have octahedrally coordinated positions in the monoclinic crystal structure. However, the low conductivity of $CoMoO_4$ and its high tendency of agglomeration cause low capacity and short cycle life. Therefore to benefit the advantages of both materials (Co and Ni) while improving the cycle life as well as the rate performance of the battery, a new electrode design is highly required.

Up to now different methods have been used to fabricate metal molybdates such as chemical reaction [5], hydrothermal/solvothermal reaction [6], microwave heating [7], chemical precipitation [8], combustion synthesis [9], sono-chemical process [10], sol-gel method [11] and solid-state methods [12]. In this sense Xiao et al have fabricated $AMoO_4$ (A: Ni, Co) nanorods by hydrothermal methods to be used as anode material in LIBs [13]. But the performance has been found to be too weak to be commercialized. Then, to improve the performance of the electrode, scientists have designed hybrid electrodes where carbon cloths/graphene layers or graphene oxide have been used as supporting structure of $NiMoO_4$ [14-15]. Then, Lyu et al [16] and Xu et al [17] have fabricated graphene wrapped $CoMoO_4$ nanospheres by hydrothermal and lotus root-like $CoMoO_4$@graphene nanofibers by electrospinning methods, respectively.

Although various strategies about optimizing the composition, the structure and the morphology of the metal molybdate powders have been studied, upto now no research has been published about the use of quaternary molybdate powders as electrodes for lithium ion batteries. Herein, Ni and Co are explicitly chosen to combine with molybdenum and oxygen not only because of their similar physical and electrochemical properties but also their structural resemblances. The fact that both Ni and Co atoms have relatively small atomic radius and relatively big electronegativity, in $AMoO_4$ (A:Ni, Co) structure Mo atoms are expected to be positioned octahedrally.

In this work hydrothermal process has been chosen as production method due to its soft chemistry which enables one to fabricate crystalline metal oxides with particular morphology and sizes [18]. And, knowing that nano-structured materials have attracted much attention, process parameters have been optimized to nanoengineer this transitional metal molybdates (not given here) to improve the electrochemical performances. Because by using nanostructured electrodes, the ion diffusion distance would be decreased, the electrolyte-electrode contact area would be increased and intergaps between the particles to maintain the electrode integrity would be promoted.

In this study first in literature, the performance of the nickel molybdate (NM) anode has been improved by two different designs: cobalt oxide decorated nickel molybdate (Co@NM) versus nickel-cobalt-molybdate (NCM) composite powders. Nickel molybdate and nickel-cobalt-molybdate composite powders have been fabricated by one-pot hydrothermal process; whilst, a combination of hydrothermal and chemical precipitation processes have been used to design cobalt oxide decorated nickel molybdate powders.

The resulting powders' properties have been analyzed morphologically, structurally and electrochemically when used as anodes in lithium ion batteries. The best performance is achieved by Co@NM powders as the cobalt oxide decoration over the nanostructured molybdate is believed to help the formation of a stable electrode/electrolyte interface while maintaining the electrode integrity upon cycling.

2. EXPERIMENT

2.1. Experimental section

Analytical grade $NiCl_2 \cdot 6H_2O$, $CoCl_2 \cdot 6H_2O$, ethanol, NH_3 and Merck quality $Na_2MoO_4 \cdot 2H_2O$ (Merck: 1.01180.0250), HNO_3 (Merck: 1.00456.2500) were used as received without any further purification. Distilled water was used in all the experiments.

The pure $NiMoO_4$ (NM) powders were synthesized via a simple one-step hydrothermal method. The typical synthetic procedure was followed by mixing equimolar ratio of $NiCl_2 \cdot 6H_2O$ and $Na_2MoO_4 \cdot 2H_2O$ in 30 ml of distilled water separately with constant stirring rate (400 rpm) at room temperature. Then, after the addition of each 30 ml solution one to another, 120 ml ethanol was added into the 60 ml of the mixture. Then, the solution was stirred for another 30 min. The pH of the solution was adjusted to 7 with HNO_3 solution. The solution obtained was then transferred to a Teflon coated stainless steel autoclave (250 ml) and kept at 150 °C for 6 h in an oven. Once it was done, the end product was collected by centrifugation (6000 rpm, 30min). Then, the product was dried overnight at 80°C and calcinated in atmospheric ambient for 2 hours at 450 °C with a heating rate of 5 °C min^{-1}.

$NiCoMoO_4$ (NCM) composite powders were synthesized following the similar one pot hydrothermal synthesis procedure that was defined above. Equimolar ratios of $NiCl_2 \cdot 6H_2O$ and $CoCl_2 \cdot 6H_2O$ were stirred in 15ml of distilled water separately. Once the nickel ion and cobalt ion containing solutions were gathered together, the mixture was stirred for 30 min. Then, first 30 ml AHM of equimolar ratio then 120 ml of ethanol were added subsequently and stirred for additional 30 min. Finally after the pH adjustment of the solution (to pH 7 by using HNO_3) the mixture was transferred into the autoclave for hydrothermal processing (150 °C, 6 hours). Once the reaction ended up, the product was separated by centrifugation (6000 rpm 30min), and the collected powder was dried (at 80 °C, overnight) and calcinated (2 hours at 450 °C).

Finally, Co oxide decorated nickel molybdate (Co@NM) powders were fabricated in two steps: firstly, NM powders were fabricated as explained above. Secondly, 0.4g NM was dispersed ultrasonically in 30 ml water at room temperature. After the addition of 20 ml water to the mixture, the temperature of the solution was increased to 60^0C. The solution was kept rigorously stirred (at 400 rpm) for 1hour. Then, 2.86g $CoCl_2.6H_2O$ was added and the mixture was stirred for an additional 1 hour. The end product was separated by centrifugation (2 times with water and ethanol, 6000 rpm 30 min) then dried (at 80°C, overnight) and calcinated (for 2 hours at 750°C with a heating rate of 5 °C min^{-1}) (see Fig.1 for detailed fabrication procedure).

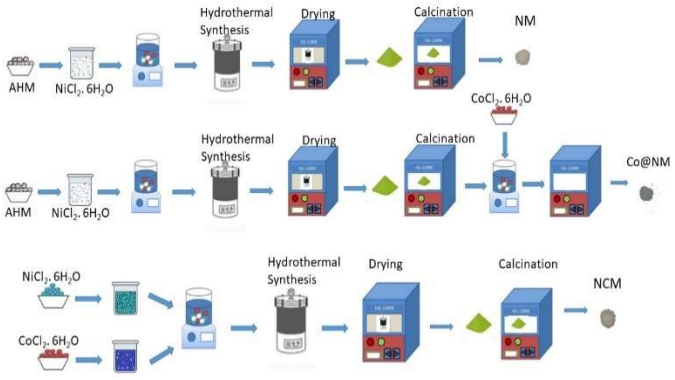

Figure 1. Schematic representation of NM, Co@NM and NCM samples

2.2. Characterization

The general morphologies of the powders and the surface views of the electrodes after cycling were characterized by scanning electron microscopy (SEM, Zeiss Gemini 500). The elemental compositions of the powders were determined by energy dispersive spectroscopy (EDS, Brucker).

The structures of the powders were determined via X-ray diffraction method (Rigaku) by using Cu Kα radiation.

2.3. Electrochemical Analysis

To evaluate the electrochemical performance of the NM, NCM and Co@NM electrodes, a typical two cell electrode configuration was used.

A standard electrolyte containing 1 M $LiPF_6$ in a mixture of ethylene carbonate (EC) and dimethyl carbonate (DMC) (1: 1 in volume) (Merck) was used in this study. The anode and the counter electrode (Lithium) were separated by a Celgard 2400 separator (Celgard Inc., USA). The CR2032-type coin cell was assembled in argon gas filled glove box (Mbraun, Labmaster) where the oxygen and the humidity levels were below 1 ppm. To measure the cycle performance of the electrodes, the samples were used as anodes and cycled between 1mV-3V vs Li/Li^+. To further improve the stability of the SEI film, 10 wt % fluorinated ethylene carbonate (FEC) was added into the standard electrolyte.

Both cyclic voltammetry (CV) and electrochemical impedance spectroscopy (EIS) were performed on Gamry Interphase 1000 electrochemical workstation. CV test was done with a scan rate of 0.1 mV s^{-1} between 0.001-3V vs Li/Li^+ for the 1^{st}, 2^{nd}, 3^{rd} and 4^{th} cycles. Electrochemical impedance spectroscopy (EIS) data was obtained after 1^{st}, 2^{nd} and 4^{th} cycles at 1mV in the frequency range of 10^5 - 0.01 Hz.

3. RESULTS AND DISCUSSION

3.1. Surface morphology and microstructure

The fabrication processes of NM, NCM and Co@NM powders are schematically depicted in Figure 1. Hydrothermal process combined with calcination is mainly used to fabricate binary (NM) and ternary (NCM) oxide powders. Post-treatments (after one pot hydrothermal process) including chemical precipitation and calcination have been used to fabricate Co@NM powders. Knowing that the pH of the precursor solution has a crucial effect on both the formation of molybdate phase and its morphology, for all samples pH is adjusted to 7 with NH_3 solution, following the suggestion of Ding et al [19].

Fig.2a-c reveal the FE-SEM images of powders. A worm-like morphology is noted for NM powders [20]. Then with the addition of Cobalt ions into the hydrothermal's precursor solution, worms' growth rate increases and NCM nanowires are fabricated. Finally when worms-like structured NM material is chemically treated via a cobalt chloride solution, then heat treated, cobalt oxide decorated NM powders are produced. The existences of Co atoms in NCM and Co@NM materials are justified by EDS analysis (Table1).

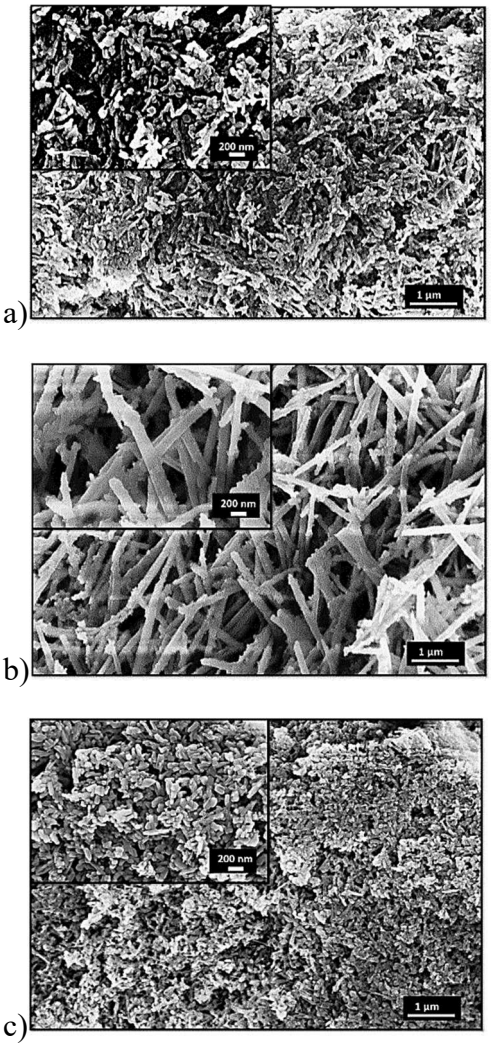

Figure 2. SEM images of a) Nickel molybdate, b) Nickel-cobalt molybdate, c) Cobalt oxide decorated

Nickel molybdate powders (upper left hand image shows 75k magnification)

When the hydrothermal process mechanism is analyzed, it is seen that at the initial stage of the reaction, during mixing of $(NH_4)_6Mo_7O_{24}$ solution with $NiCl_2 \cdot 6H_2O$, a supersaturated solution is formed with plenty of tiny crystallites. The latter is believed to work as nucleation centers and serves as the nuclei for the growth of self-assemblies made of Ni^{2+} and MoO_4^{2-} ions. The shape of these self-assemblies is similar to 'worm' [2, 15]. Then, with the addition of $CoCl_2.6H_2O$ into the precursor solution, Co atoms are deposited along with Ni and Mo stochiometrically and worms transform into nanowires forming NCM nanocomposite powders. Finally, the chemical-treatment of NM worms via a $CoCl_2.6H_2O$ solution, followed by the heat treatment process leads decoration of NM powders by cobalt oxide particles (Figs 2a-c).

Table 1. EDS analysis results of samples (at%)

Sample Code	O	Ni	Mo	Co
NM	68	16	15	-
NCM	68	8	15	8
Co@NM	66	16	16	2

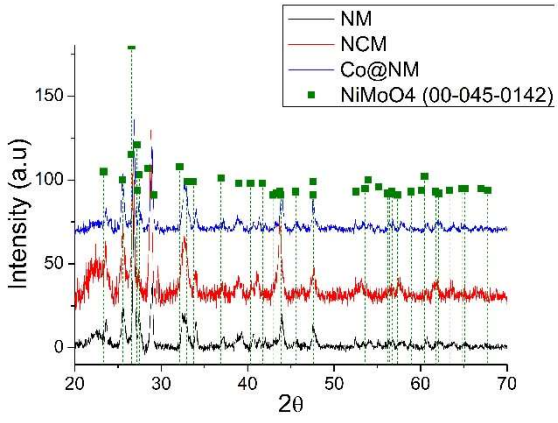

Figure 3. XRD results of NM, NCM and Co@NM powders.

Fig.1 shows that the color of the powder changes depending on their compositions and crystal structures. Hex color codes define the colors as light yellow for NM, dim gray for NCM and dark slate gray for Co@NM. The crystallographic structure and phase purity of the samples are analyzed by powder XRD method. Fig 3 shows that all three samples reveal peaks at 29.1^0 and 32.1^0 proving the existence of the nickel molybdate. Herein as the $CoMoO_4$ and $NiMoO_4$ have very similar crystallography (they both have monoclinic structure), their peaks are found to be overlapped in most case (not shown here). The absence of cobalt oxide peaks, bump at low diffraction angle and the enlargement of peaks could be related to the nanocrystalline size and/or amorphous structure of the cobalt oxide particles in NCM and Co@NM powders.

3.2. Electrochemical performance analysis

In order to improve the electrochemical performance of the electrode, one promising way is to develop a novel hybrid material by combining the metal oxides with binary metal molybdates since the capacitance of the anode is largely determined by the chemical and structural stabilities of the material during cycling.

Previous studies about the lithiation mechanism of molybdates have shown that an irreversible phase transformation (through an intermediate product transformation into an amorphous lithiated material) occurs in the 1st discharge reaction. When the capacity-cycle curve of $MnMoO_4$ is observed, Kim et al have noted an initial discharge capacity which couldn't be explained by the valence change in Mo. Therefore, possible oxygen contribution into the lithiation reaction along with Molybdenum is believed to be the reason for that [21]. Indeed, anion contribution to the charge compensation has been discussed previously. Denis et al. [22] have mentioned that although Mo-O bond has strong covalent character lithium reduction and partial oxidation is found to occur with oxygen.

Herein, to examine the lithiation mechanism of the NM, NCM and Co@NM samples, CV tests have been applied during the initial 4 consecutive cycles (Figs.4a-c). In the first cathodic scan, two remarkable cathodic peaks at around 0.75 and 0.2 V with a bump around 1.6 V are detected for NM electrode. Those peaks show the electrochemical

reduction of NM to metallic Ni and Mo, with the decomposition of the organic electrolyte to form a solid-electrolyte interface (SEI). In the first anodic scan, one remarkable peak at 1.7V is noted, which depicts the oxidation of Ni and Mo to Ni^{+2} and Mo^{+6} respectively [15]. After 1st cycle, the cathodic peak at 1.6 V is shifted to lower potential, due to reversible reduction reaction of MoO_3 and NiO to Mo and Ni metal, respectively. It is important to note that the integral areas are almost constant from 2nd to 4th cycles showing the good reversibility of the reaction. For NCM and Co@NM electrodes, first cycle CV curvatures demonstrate similar peaks, whilst their intensities are lower than that of NM electrode. The comparison of the 1st cycle CV curvatures of three samples reveals that Cobalt oxide decoration on NM electrode causes a shift of the cathodic peak at 0.7 V to lower potentials. Then, this cathodic bump at 0.7 V will be appeared after 2nd cycle and remains until 4th cycles, like NM and NCM electrodes. This fact highlights the importance of material science on the battery technology since not only the composition but also the design of the electrode material affects the lithiation reaction, hence the electrochemical performance remarkably.

On the basis of CV curvatures (Figs.4a-c) and literature review the electrochemical reaction of the NM, NCM and Co@NM electrodes in cycling can be described as follows (Eqs. 1-6) [15] (M: Ni or Co)

$$MMoO_4 + 8Li^+ + 8e^- \rightarrow M + Mo + 4Li_2O \quad \text{(Eq1)}$$

$$M + Li_2O \rightarrow MO + 2Li^+ + 2e^- \quad \text{(Eq2)}$$

$$Mo + 3Li_2O \rightarrow MoO_3 + 6Li^+ + 6e^- \quad \text{(Eq3)}$$

$$M + Mo + 4Li_2O \leftrightarrow Mo + MoO_3 + 8Li^+ + 8e^- \quad \text{(Eq4)}$$

$$Ni_xCo_{1-x}MoO_4 + 8Li^+ + 8e^- \rightarrow xNi + (1-x)Co + Mo + 4Li_2O \quad \text{(Eq5)}$$

$$xNi + (1-x)Co + Mo + 4Li_2O \leftrightarrow xNiO + (1-x)CoO + MoO_3 + 8Li^+ + 8e^- \quad \text{(Eq6)}$$

Figs 5a gives the capacity-cycle performance of NM, NCM and Co@NM samples. The fact that all samples perform 100 cycles test without failure, it proves that nanostructuring is a good approach for designing electrode material. NM electrode has the weakest performance. The latter highlights the importance of cobalt atoms for anode material, as stated Yang et al [2]. Despite the worm-like morphology of NM which leads open spaces in the electrode and higher specific surface area with short ion/electron diffusion, insufficient structural stability causes rapid capacity fade. Plus, the dead surface of the PVDF binder limits the reversibility of the electroactive NM as the particles aggregate and expand in cycling, hence possible partial delamination may occur upon cycling.

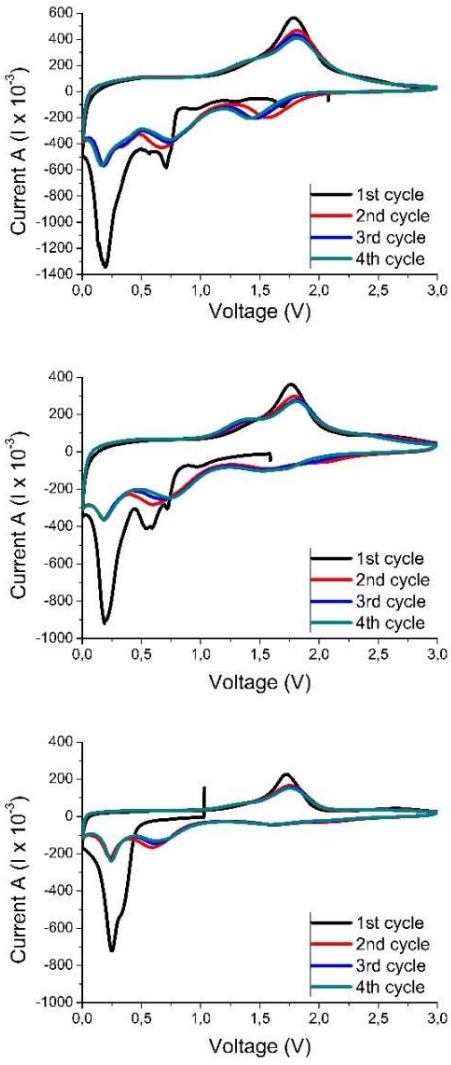

Figure 4. 1st, 2nd, 3rd and 3th cycles CV curves of a) NM, b) NCM, c)Co@NM electrodes

Figure 5a depicts that the composite (NMC) electrode reveals a progressive decrease in the capacity. Possible fractures releasing new electrode's surfaces that will be exposed to the electrolyte at each successive cycle is believed to cause irreversible electrochemical reactions, leading thicker SEI film formation.

Finally the capacity-cycle performance of Co@NM electrode is found to be better than others as it gets stabilized after initial cycles (Fig.5a). Indeed, although the morphology of Co@NM is very similar to that of NM, the superior electrochemical performances of the Co@NM nanostructures could be related to the poor crystallinity of the cobalt oxide particles that decorate NM powders to improve the transportation, and electrochemical stabilizing effect. When Li intercalates into the particle, volume expansion occurs as expected. And, the differences in the lithiation kinetics and the extents of volume expansion for Nickel molybdate and cobalt oxide cause a cover formation on the electrode surface which promotes stable electrode/electrolyte interface.

Then, to further test the effect of FEC addition into the molybdates electrode's performance, 10%FEC (fluoroethylene carbonate) is added into the standard electrolyte and the Co@NM electrode is tested galvanostatically for 200 cycles. Fig.5b shows that independent of the electrolyte composition, the Co@NM electrode performs similar first discharge and 1st coulombic efficiency (around 1100mAh/g with 40% coulombic efficiency), but the capacity retention changes. The Co@NM electrode delivers 230 mAh/g after 100 cycles and 220 mAh/g capacity after 220 cycles in the case of the FEC addition; whilst it delivers 280 mAh/g after 100th cycles when it is tested with the standard electrolyte. Thicker SEI formation induced by FEC addition is believed to restrict lithiation of active particles. Thus, the amount of FEC which is added into the electrolyte could be optimized to improve the capacity retention of the electrode, in future studies.

Fig. 5c gives the result of the Co@NM electrode's rate performance. The result clearly shows that Co@NM electrode can cycle even at high rates (upto 700mA/g). Yang et al [2] have claimed that good rate capability of the electrode is mostly contributed to its Co content.

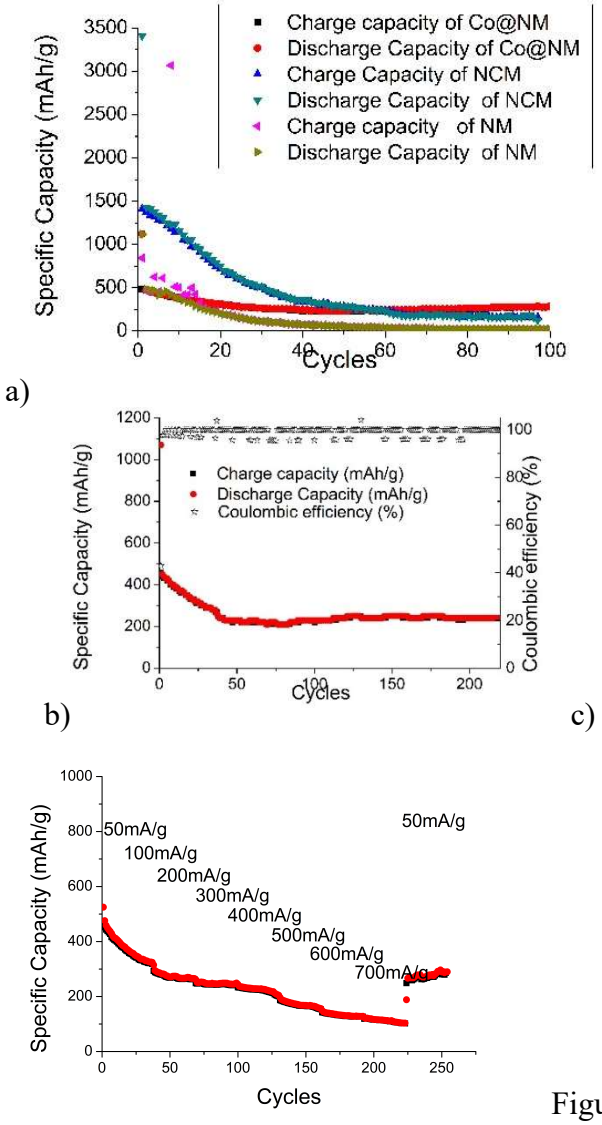

Figure 5. Capacity-cycle performance of a) NM, NCM and Co@NM electrodes, b) Co@NM with 10%FEC addition into the electrolyte, c) Rate performances of Co@NM electrodes

To get more understanding about the lithiation mechanism of the NM, NCM and Co@NM samples, EIS test has been applied after 1st, 2nd and 4th cycles when the electrode is discharged to 1mV (Figs.6a-c). As demonstrated in Figures 6a-c, the Nyquist plots of the electrodes are composed of a semicircle in high frequency region, a semicircle in middle frequency region and a sloped line in low frequency region. The

ohmic resistance that is noted at high frequencies is related to the external cell connection and the electrolyte resistance. This value is found to be very small for all samples which shows that the battery is well assembled. Semicircles noted in the high and middle frequency regions are related to solid electrolyte interphase (SEI), and charge transfer reactions of the electrode, respectively. Finally, the sloped line detected in the low frequency region depicts the solid-state lithium ions diffusion into the active material. All data given on the Nyquist plots agrees with Kramers–Kronig (KK) relation which is used to validate the EIS data.

The comparison in the Nyquist plots of each sample from 1st to 4th cycles depicts some changes in the electrode/electrolyte interphase upon cycling: the diameter of the semi-circle related to the charge-transfer resistance decreases. An induced electrochemical activity of each electrode after 1st cycle and/or possible morphological changes of the active particles (electrochemical pulverization) decreasing the particle size may elucidate this outcome [23].

To evaluate the validity of the proposed lithiation mechanism the cells containing NCM and Co@NM electrodes are disassembled after cycles in the glovebox and washed with DMC before drying in oxygen free atmosphere. Post-SEM analysis reveals no delamination and/or peel-off. Pulverization is noted for each sample. This observation supports electrochemical test results (Figs. 4-6). A scrutiny look in Figs.7a-b shows that NCM has some cracks in the electrode; whilst, Co@NM has no remarkable cracking. A homogeneous blurry surface appearance is noted on Fig.7. This shows that although pulverization happens in the electrode, cobalt oxide coating over nickel molybdate works as a cover onto the electrode. It provides more stable electrode/ electrolyte interface eventually. Therefore, this paper substantiates that for the optimization of the electrode's electrochemical performance, the development of a novel hybrid electrode material represents a good solution. Because, by combining the metal oxide with binary metal molybdates, the electrode performs more stable lectrode/electrolyte interface in cycling, hence longer cycleability.

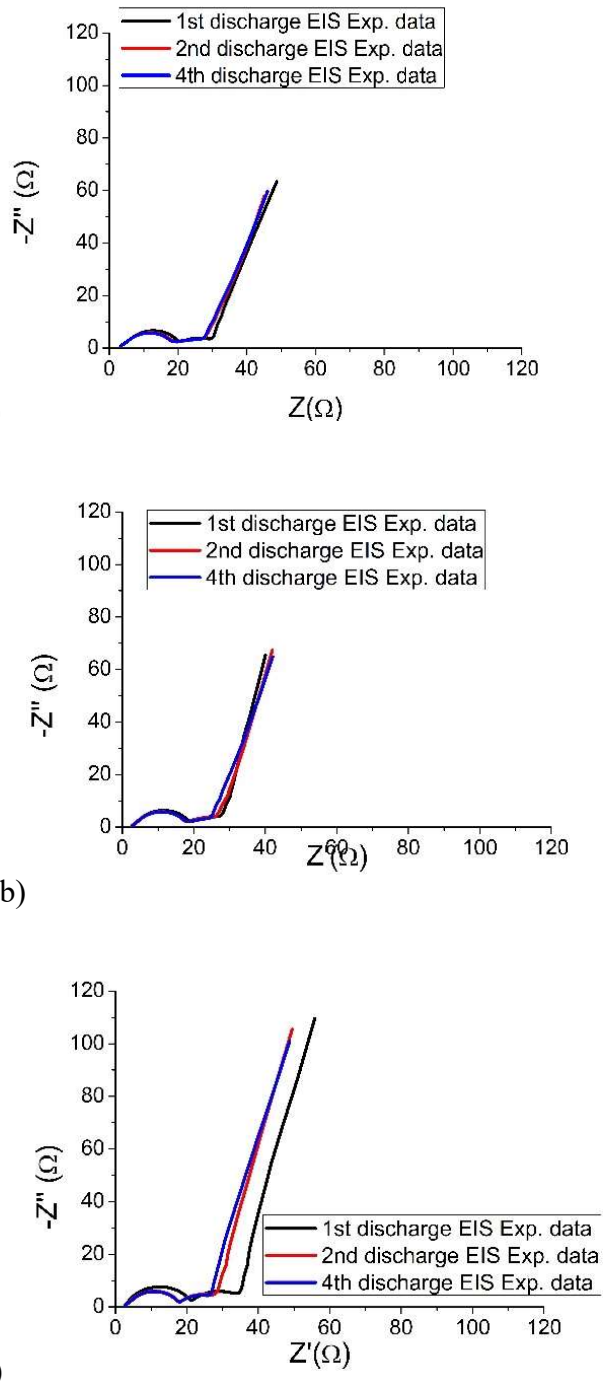

Figure 6. EIS test results a) NM, b) NCM, c) Co@NM electrodes.

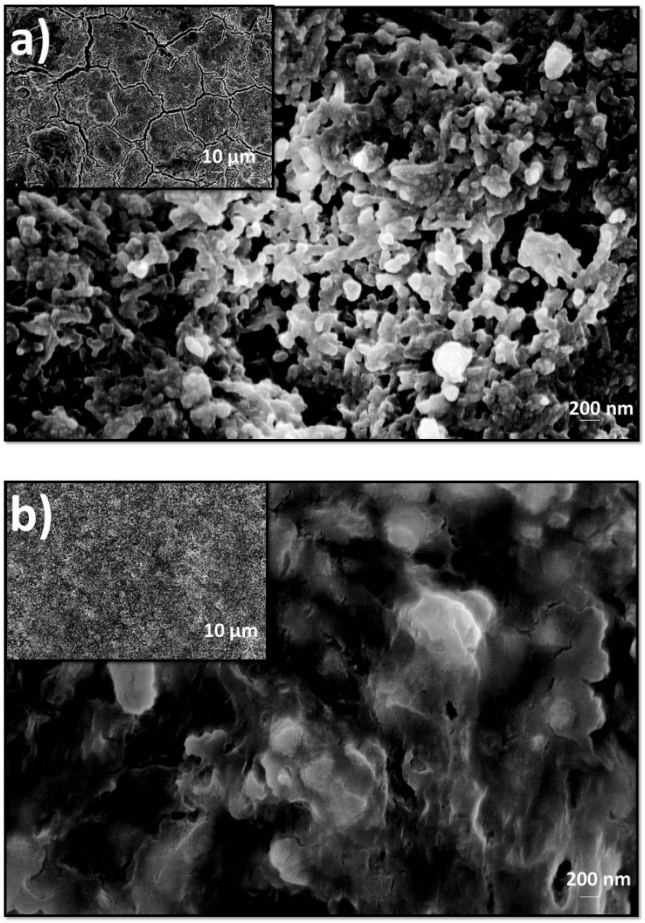

Figure 7. Post SEM analysis of a)NCM, b)Co@NM electrodes.

4. CONCLUSION

This paper focus on the characterization of the differently fabricated nickel-cobalt-molybdenum containing oxide powders and the evaluation of their performances when used as negative electrodes in lithium ion batteries.

Within the scope of the paper, importances of electrode morphology, structure and composition have been discussed. Moreover, the electrolyte/electrode interaction has been investigated. The results can be summarized as follows:

-Processes have been design to fabricate differently structured powders: Nickel-cobalt composite molybdate (NCM) and nickel molybdate ternary oxide powders (NM) are fabricated by conventional hydrothermal method. The cobalt oxide decorated nickel molybdate powders (Co@NM) are synthesized by a combination of hydrothermal and chemical precipitation methods.

- The advantage of nanoengineering has been approved since no early faillure has been noted in galvanostatic tests. It is believed that 1D structure enhances faster Li ion diffusion along the structure. Plus, the open spaces among them is expected to promote electrolyte-electrode interaction. Therefore the electrolyte that penetrates more into the electrode would find more active particles to react with. Additionally, these spaces create more available area to accomodate volume expansion that occur in cycling.

- The positive effect of Co addition into and onto the Nickel molybdate electrode's electrochemical performance has been demonstrated by capacity-cycle curves. The comparison of NCM and Co@NM electrodes' performances reveal differences. The latter highlights the importance of the electrode design along with its composition.

- The capacity retention of the Co@NM electrode over 220cycles has been measured by adding 10%FEC into the standard electrolyte. The results show that %FEC addition doesnot have a distinguished positive effect on the first cycle performance of Co@NM electrode. An optimization of FEC content could be studied in future to ameliorate the capacity retention of the electrode.

- The rate performance of the electrodes show that Co@NM electrode keeps cycling even at 700mA/g rate and it delivers 200mAh/g capacity under a current load of 400mA/g.

- Post-SEM analysis' results agree with galvanostatic and electrochemical test' (Cv and EIS) outcomes. They all show that Co@NM electrode exhibits better electrochemical performance due to stabilized electrode/electrolyte interface. NCM electrode

reveals some cracking causing a progressive decrease in the capacity.

5. REFERENCES

[1] C. T. Cherian, M. V. Reddy, S. C. Haur, B. V. R. Chowdari "Interconnected Network of $CoMoO_4$ Submicrometer Particles As High Capacity Anode Material for Lithium Ion Batteries," ACS Appl. Mater. Interfaces, vol. 5, pp. 918−923, 2013.

[2] Q.Yang, S.-Y. Lin, "Rationally designed nanosheet-based $CoMoO_4$–$NiMoO_4$ nanotubes for high-performance electrochemical electrodes," RSC. Adv., vol.6, pp. 10520-10526, 2016.

[3] N.N. Leyzerovich, K.G. Bramnik, T. Buhrmester, H. Ehrenberg, H. Fuess, "Electrochemical intercalation of lithium in ternary metal molybdates $MMoO_4$ (M: Cu, Zn, Ni and Fe)," J. Power Sources, vol. 127, pp. 76–84, 2004.

[4] P. R. Jothi, K. Shanthi, R. R. Salunkhe, M. Pramanik, V. Malgras, S. M. Alshehri, Y. Yamauchi "Synthesis and Characterization of α-$NiMoO_4$ Nanorods for Supercapacitor Application," Eur. J. Inorg. Chem., pp. 3694–3699, 2015.

[5] S.-S. Kim, S. Ogura, H. Ikuta, Y. Uchimoto, M. Wakihara "Reaction mechanisms of $MnMoO_4$ for high capacity anode material of Li secondary battery," Solid State Ionics, vol. 146, pp. 249–256, 2002.

[6] 6. D. Zhang, R. Zhang, C. Xu, Y. Fan, B. Yuan, "Microwave-assisted solvothermal synthesis of nickel molybdate nanosheets as a potential catalytic platform for NADH and ethanol sensing" Sens. Actuators B, vol. 206, pp. 1–7, 2015.

[7] H. Wan, J. Jiang, X. Ji, L. Miao, L. Zhang, K. Xu, H. Chen, Y. Ruan, "Rapid microwave-assisted synthesis $NiMoO_4 \cdot H_2O$ nanoclusters for supercapacitors," Mater. Lett. Vol. 108, pp. 164–167, 2013.

[8] 8. M. C. Liu, L. B. Kong, C. Lu, X. J. Ma, X. M. Li, Y. C. Luo, L. Kang, "Design and synthesis of $CoMoO_4$–$NiMoO_4 \cdot xH_2O$ bundles with improved electrochemical properties for supercapacitors," J. Mater. Chem. A, vol.1, pp. 1380–1387, 2013.

[9] S. Vidya, S. Solomon, J. K. Thomas, "Single step combustion synthesis of nanocrystalline scheelite $Ba_{0.5}Sr_{0.5}MoO_4$ for optical and LTCC applications: Its structural, optical and dielectric properties," J. Electroceramics vol.36, pp.142-149, 2016.

[10] M. P.-Kalamuei, M. M.-Kamazani, M. S.-Niasari,S. M. H.-Mashkani, "A simple sonochemical approach for synthesis of selenium nanostructures and investigation of its light harvesting application," Ultrason. Sonochem., vol 23, pp.246-256, 2015.

[11] M. Devi, U. V. Varadaraju, "Lithium insertion in lithium iron molybdate," Electrochem. commun., vol.18,pp.112-115, 2012

[12] M. Zhou, X. Jiang, C. Li, Z. Lin, J. Yao, Y. Wu, "The Double Molybdate $Rb_2Ba(MoO_4)_2$: Synthesis, Crystal Structure, Optical, Thermal, Vibrational Properties, and Electronic Structure," Z. Anorg. Allg. Chem., vol.641, 2321-2525, 2015

[13] W. Xiao, J. S. Chen, C. M. Li, R. Xu, X. W. Lou "Synthesis, Characterization, and Lithium Storage Capability of $AMoO_4$ (A = Ni, Co) Nanorods, " Chem. Mater., vol. 22, pp.746–754, 2010.

[14] X. Li, J. Bai, H. Wang, "Synthesis of hierarchical free-standing $NiMoO_4$/reduced graphene oxide membrane for high-performance lithium storage," J Solid State Electrochem., vol. 22, pp. 2659–2669, 2018.

[15] B. Wang, S. Li, X. Wu, W. Tian, J. Liu, M. Yu "Integration of network-like porous $NiMoO_4$ nanoarchitectures assembled with ultrathin mesoporous nanosheets on three-dimensional graphene foam for highly

reversible lithium storage," J. Mater. Chem. A, vol.3, pp. 13691-13698, 2015.

[16] D. Lyu, L. Zhang, H. Wei, H. Geng, H. Gu "Synthesis of graphene wrapped porous $CoMoO_4$ nanospheres as high-performance anodes for rechargeable lithium-ion batteries" RSC Adv., vol. 7, pp. 51506–51511, 2017.

[17] J. Xu, S. Z. Gu, L. Fan, P. Xu and B. G. Lu, "Electrospun Lotus Root-like $CoMoO_4$@Graphene Nanofibers as High-Performance Anode for Lithium Ion Batteries," Electrochim. Acta, vol. 196,pp. 125–130, 2016.

[18] K. Schuh, "Hydrothermal synthesis of molybdenum based oxides for the application in catalysis," Dissertation, Karlsruher Institut für Technologie, 2014.

[19] Y. Ding, Y. Wan, Y.-L. Min, W. Zhang, S.-H. Yu "General Synthesis and Phase Control of Metal Molybdate Hydrates $MMoO_4 \cdot nH_2O$ (M:Co, Ni, Mn and n:0, 3/4, 1) Nano/Microcrystals by a Hydrothermal Approach: Magnetic, Photocatalytic, and Electrochemical Properties," Inorganic Chem., vol.47, pp.7813-7823, 2008.

[20] X. Tian, X. Li, T. Yang, K. Wang, H. Wang, Y. Song, Z. Liu, Q. Guo, "Porous worm-like NiMoO4 coaxially decorated electrospun carbon nanofiber as binder-free electrodes for high performance supercapacitors and lithium-ion batteries," Appl. Surface Science, vol. 434 pp.49–56, 2018.

[21] S.-S.Kim, S. Ogura, H. Ikuta, Y. Uchimoto, M. Wakihara, "Reaction mechanisms of $MnMoO_4$ for high capacity anode material of Li secondary battery," Solid State Ionics, vol. 146, pp.249–256, 2002.

[22] S. Denis, E. Baudrin, M. Touboul, J.-M. Tarascon, "Synthesis and Electrochemical Properties of Amorphous Vanadates of General Formula RVO_4 (R = In, Cr, Fe, Al, Y) vs. Li," J. Electrochem. Soc., vol.144, pp.4099-4109, 1997.

[23] C. Tan, J. Cao, A. M. Khattak, F. Cai, B. Jiang, G. Yang, S. Hu "High-performance tin oxide-nitrogen doped graphene aerogel hybrids as anode materials for lithium-ion batteries," J. Power Sources, vol. 270, pp. 28-33, 2014.